P2.33 MODELING THE DIURNAL CYCLE OF SHALLOW CONVECTION AND CLOUDINESS IN TRADE WIND BOUNDARY LAYER OVER THE INDIAN OCEAN

Hailong Wang* and Greg M. McFarquhar

University of Illinois, Dept. of Atmospheric Sciences, Urbana, Illinois

1. INTRODUCTION

Most previous large-eddy simulation (LES) studies of trade wind cumuli (Sommeria 1976; Stevens et al. 2001; Siebesma et al. 2003) have examined shallow convection under undisturbed conditions, where constant radiative forcing and surface fluxes were assumed. As a consequence, thermodynamic and cloud fields reached a quasi-steady state. However, both observations (e.g., Brill and Albrecht 1982; Wood et al. 2002) and modeling studies (e.g., Ackerman et al. 2000; Johnson 2005; McFarquhar and Wang 2006) show that cloudiness in the trade wind boundary layer has a significant diurnal variation driven by diurnally varying external forcings.

The external forcings acting on the trade wind boundary layer include solar radiative forcing, surface fluxes and large-scale forcing. In this study it is examined how these forcings drive the diurnal cycles of shallow convection and cloudiness. Using a one-dimensional trade-wind boundary layer model, Brill and Albrecht (1982) previously found that solar radiative heating in clouds primarily produced the diurnal variation. A three-dimensional LES model, which more realistically represents the physical processes in the trade-wind boundary layer, was used here to gain a better understanding of the changes in the temperature and moisture structure, circulations and turbulent fluxes induced by the diurnally varying solar radiation.

2. MODEL DESCRIPTION AND INITIALIZATION

The model used for this study was the non-hydrostatic Eulerian/semi-Lagrangian (EULAG) model (Smolarkiewicz and Margolin 1997). McFarquhar and Wang (2006) describe the settings and initialization of the model. Simulations with 100 m horizontal and 40 m vertical resolution were performed in a 40 km^2 by 3 km domain. The input environmental profiles were derived from dropsonde measurements made during the Indian Ocean Experiment (INDOEX) using a technique that preserved the average heights of the mixed layer, the conditionally unstable layer and the trade wind inversion (MaFarquhar and Wang 2006). Figure 1 shows profiles of potential temperature, water vapor mixing ratio and wind measured on 24 February 1999 in conditions identified by McFarquhar et al. (2004) as pristine. A well-mixed layer existed in the lower 0.5 km below a conditionally unstable layer that extended to 1.5 km.

* *Corresponding author address:* Hailong Wang, University of Illinois, Dept. of Atmospheric Sciences, 105 S. Gregory Street, Urbana, IL, 61801-3070, e-mail: hailong@atmos.uiuc.edu.

The trade inversion was not as strong as those in soundings used to initialize other LES simulations (Ackerman et al. 2000; Stevens et al. 2001; Siebesma et al. 2003). The wind speed had a maximum of 6.5 ms^{-1} at the inversion base. Sea surface temperatures (SSTs) were estimated using retrievals from the Tropical Rainfall Measuring Mission (TRMM) microwave imager (TMI). Vertical velocity profiles obtained from the European Center for Medium-range Weather Forecasts (ECMWF) analysis over the INDOEX domain were used as a large-scale forcing term.

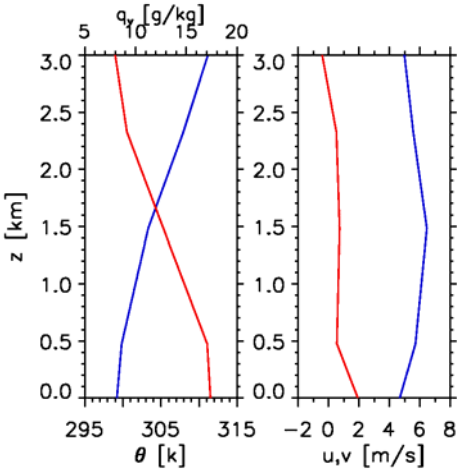

Figure 1 Initial profiles of potential temperature θ (blue), water vapor mixing ratio q_v (red), and the wind components u (blue) and v (red).

3. EXPERIMENTS AND SIMULATION RESULTS

3.1 Diurnal Variation Statistics

In a control experiment (CON), solar radiative forcing varied diurnally in the model atmosphere, and surface fluxes and cloud radiative effects were computed interactively. No large-scale forcing was applied. Figure 2 shows the 24-hour time series of domain averaged cloud water mixing ratio q_c. Periodic pulsations were superimposed on the diurnal cycle of q_c. To obtain the dominant period of these pulsations, a fast Fourier transform (FFT) analysis was applied to the time series. The resulting power spectrum is shown in Figure 3. Frequency peaks of around 1.97x10^{-4} sec^{-1}, 1.74x10^{-4} sec^{-1} and 1.15x10^{-5} sec^{-1} correspond to time periods of 1.4, 1.59 and 24 hours, respectively. The 24-hour period indicates the diurnal cycle illustrated by the polynomial fit. The same analysis was applied to time series of

updrafts and turbulence fluxes of moisture and buoyancy. Similar dominant frequencies were derived. The correlation coefficient of any two quantities was over 0.85.

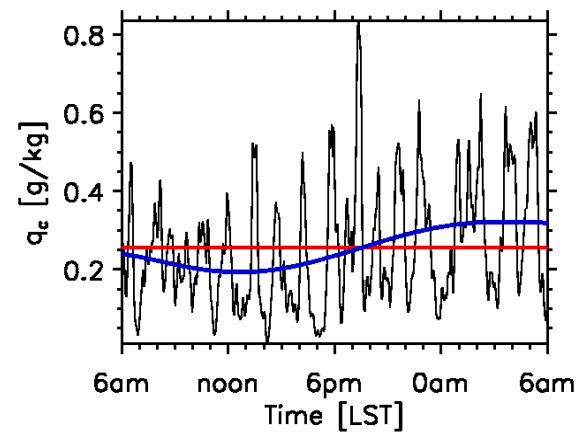

Figure 2 Time series of domain averaged q_c (black) with the daily mean (red) and a least-square polynomial fit (blue).

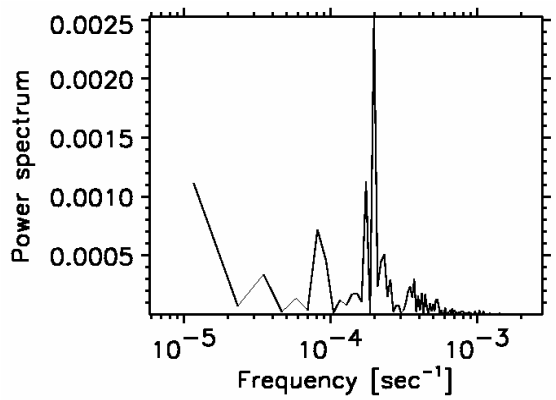

Figure 3 The power spectrum of q_c time series shown in Fig. 2 .

The diurnal cycle of cloud fraction and liquid water path (LWP) simulated in CON is shown in Figure 4. A 6-hour central moving average was applied to reduce the pulsations shown in Fig. 2. The average daytime cloud fraction and LWP were 13% and 24% lower than nighttime. The average daytime buoyancy flux, cloud mass flux and moisture flux in the conditionally unstable layer were also 47%, 32% and 33% less than the corresponding nocturnal average. As a result, the average condensation rate during the day was 38% less than that at night. The diurnal variation and vertical structure of updrafts and turbulent fluxes will be presented at the conference to illustrate the relationship between turbulent fluxes and cloud properties.

A series of sensitivity experiments were conducted to quantify the impact of surface sensible and latent heat fluxes, large-scale vertical motion, cloud radiative effects and solar heating due to non-gray gases on the diurnal cycle of shallow convection and cloudiness.

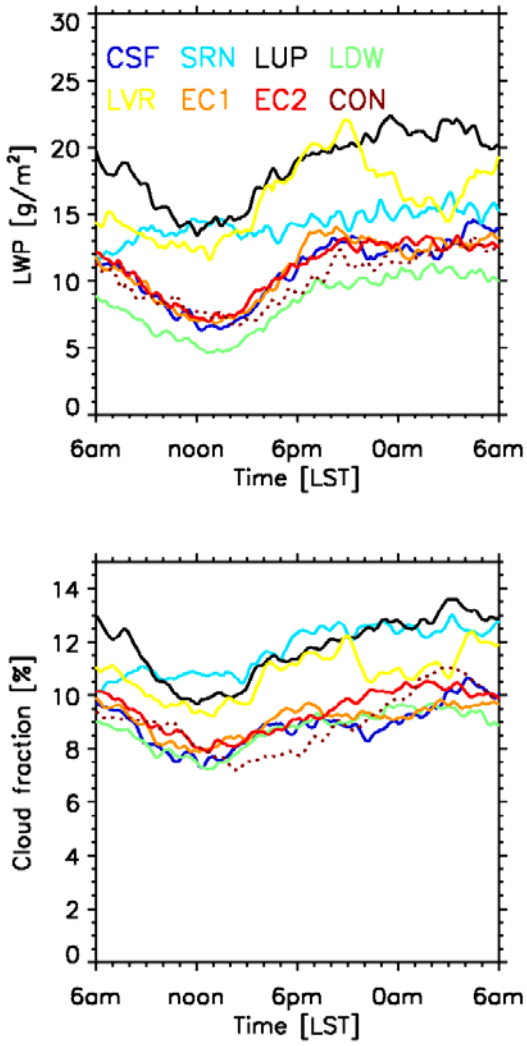

Figure 4 Diurnal variations of LWP and cloud fraction for experiment CON (dotted lines) and various sensitivity simulations indicated by the names in color.

3.2 The Role of Surface Fluxes and Large-scale Vertical Velocity

In experiment CON, the surface fluxes varied diurnally because of changes in temperature and moisture near the ocean surface. In turn, surface fluxes influenced the temperature, moisture and updrafts, and therefore, cloud properties. To examine the role of the diurnal variation of surface fluxes on the diurnal variation of cloud properties, experiment CSF prescribed constant surface fluxes given by the daily average fluxes in CON. In experiment CSF (Fig. 4) the daytime mean LWP (cloud fraction) relative to the nocturnal mean was reduced by 28% (12%), which is comparable to the 24% (13%) reduction in CON. This indicates that the diurnal variation of surface fluxes did not force the diurnal variation of shallow convection and cloudiness. The other sensitivity studies described

below also assume the same constant surface fluxes. Otherwise, any changes in surface fluxes induced by different temperature and moisture fields near the surface could impact the cloudiness.

Large-scale vertical motion can affect the vertical structure of the marine boundary layer and hence the cloud properties. In experiment LDW a constant subsidence profile was prescribed as the daily mean of the negative ECMWF large-scale vertical velocities, while in experiment LUP a constant ascent profile was prescribed as the daily mean of positive velocities. The large-scale subsidence stabilized the boundary layer and suppressed the height to which cloud top grew. On the contrary, large-scale ascent deepened the boundary layer and led to a higher cloud top. As shown in Fig. 4, although the magnitude of LWP and cloud fraction in LUP and LDW changed, the pattern of diurnal cycles was similar to that in experiment CSF. In experiment LVR, a diurnally varying large-scale vertical velocity profile based on ECMWF analysis was prescribed. Unlike LUP and LDW, the pattern of diurnal variations in LVR was significantly different from CSF. The ascent or subsidence of air masses due to varying meteorological conditions larger than the model domain size can dominate the diurnal variation of cloudiness.

3.3 Radiative Effects of Cloud and Water Vapor in Cloud

In the daytime, cloud water and water vapor in cloud have critical interactions with solar radiation, giving different radiative heating profiles from those observed in nighttime. Gary and Jacobson (1977) and Randall et al. (1991) suggested that cloud radiative effects were responsible for the observed diurnal cycles of deep oceanic convection. Brill and Albrecht (1982) found that solar heating took place within trade cumuli and the resulting changes in stability triggered feedback effects leading to the diurnal variation.

To examine the radiative effects of cloud water and vapor on diurnal cycles of cloudiness, experiment EC1 and EC2 excluded the impact of cloud water on radiative fluxes. In EC2, q_v was also fixed at its initial profile to exclude the effect of horizontal inhomogeneities of q_v on radiative heating. The diurnal cycles in EC1, EC2 and CSF (Fig. 4) were very similar, showing that the radiative effects due to cloud water and the inhomogeneous moisture field did not drive the diurnal cycles. This is probably due to the small fractional coverage of trade cumuli, so that the solar heating in the upper part of clouds had an insignificant effect on the development of trade wind boundary layer. This result with regard to the role of cloud radiative effects is inconsistent with Brill and Albrecht's (1982) conclusion.

3.4 Impacts of Solar Heating

Solar radiation can also be absorbed by non-gray gases and absorbing aerosols, heating the atmosphere. In this study, aerosols were assumed to be non-absorbing so that the solar heating in the clear sky was entirely due to non-gray gaseous absorption. Nocturnal shallow convection was simulated in experiment SRN. No distinct diurnal cycle in LWP and cloud fraction was seen (Fig. 4). The constant increase of cloudiness with time was due to net radiative cooling of the atmosphere. Three idealized experiments were conducted to study the impacts of solar heating above (SRA), within (SRW) and below (SRB) the conditionally unstable layer on the turbulence, circulation and cloudiness. In these experiments diurnally varying solar heating due to clouds and gases was allowed in the appropriate layer. Compared to simulation SRN, the updrafts and turbulent fluxes were stronger throughout the boundary layer in SRB, resulting in more and higher clouds. On the contrary, in simulation SRW the updrafts were weaker in the conditionally unstable layer and the turbulence was suppressed. In SRA the updrafts and turbulent fluxes in the inversion layer and the upper part of conditionally unstable layer were weakened and the overshooting of cumulus into the inversion layer was suppressed. These results are consistent with the findings of McFarquhar and Wang (2006).

In CON solar heating above the conditionally unstable layer partly offset the daytime longwave cooling by 3.3 K day^{-1}. Hence, thermals of cool air sinking from and cumulus updrafts to the inversion layer were suppressed. Heating below the conditionally unstable layer warmed the lower boundary layer at a rate of 1.8 K day^{-1} and enhanced thermal updrafts in this layer by 12%, which accelerated the recovery of cloudiness in the late afternoon. The solar heating rate of 2.3 K day^{-1} in the conditionally unstable layer not only weakened circulations driven by cumulus updrafts, where the daytime average value was reduced by 16%, but also reduced the environmental relative humidity.

4. CONCLUSIONS

For the trade wind boundary layer with a weak capping inversion over the Indian Ocean, the simulated diurnal cycles of shallow convection and cloudiness were characterized by a nocturnal and early morning maximum and a midday minimum. Periodic pulsations with peak frequencies of 1.97×10^{-4} and 1.74×10^{-4} sec^{-1} were superimposed on a 24-hour diurnal cycle.

A simulation with constant surface sensible and latent heat fluxes and a simulation excluding the radiative effects of cloud water showed similar diurnal cycles, suggesting that these factors were not the principal cause of the diurnal cycles. The solar heating induced warming of the inversion layer and stabilizing of the conditionally unstable layer contributed to the diurnal cycles. Heating in the conditionally unstable layer not only suppressed turbulence but also reduced the environmental relative humidity, highly decreasing the possibility of condensation. Heating in the inversion layer suppressed turbulence too. Stronger thermal updrafts and turbulent fluxes in the mixed layer triggered the recovery of cloudiness in the late afternoon when the stability in the conditionally unstable layer decreased.

Depending on its direction and magnitude, large-scale vertical motion can either enhance or eliminate the

daytime reduction of cloudiness. A diurnally varying large-scale vertical velocity can drive the diurnal variation of cloudiness but it is not necessarily the same pattern as that driven by solar forcing.

5. ACKNOWLEDGEMENTS

The authors acknowledge Dr. W. Grabowski for his help with the EULAG model. This work was supported by the National Aeronautics and Space Administration (NASA) grants *NASA NAG 5-11756* and *NNG06GB92G*. The dropsonde data were obtained from NCAR's Joint Office of Science Support (JOSS); A. Heymsfield was the PI for these data during INDOEX. NASA's TRMM science team provided TMI data. The ECMWF meteorological products for INDOEX geographical area were obtained via the Laboratoire de Meteorologie Dynamique (LMD), Palaiseau, France.

6. REFERENCES

Ackerman, A.S., O.B. Toon, D.E. Stevens, A.J. Heymsfield, V. Ramanathan, and E.J. Welton, 2000: Reduction of tropical cloudiness by soot. *Science*, **288**, 1042-1047.

Augstein, E., H. Schmidt, and F. Ostapoff, 1974:The vertical structure of the atmospheric planetary boundary layer in undisturbed trade wind over the Atlantic Ocean. *Bound. Layer Meteor.*, **6**, 129-150.

Brill, K., and B. A. Albrecht, 1982: Diurnal variations of the trade-wind boundary layer. *Mon. Wea. Rev.,* **110**, 601–613.

Gray, W.M., and R.W. Jacobson Jr., 1977: Diurnal variation of deep cumulus convection. *Mon. Wea. Rev.*, **105**, 1171-1188.

Johnson, B. T., 2005: Large-eddy simulations of the semidirect aerosol effect in shallow cumulus regimes. *J. Geophys. Res.*, **110**, D14206, doi:10.1029/2004JD005601.

McFarquhar, G.M., S. Platnick, L. Di Girolamo, H. Wang, G. Wind, and G. Zhao, 2004: Trade wind cumuli statistics in clean and polluted air over the Indian Ocean from in situ and remote sensing measurements, *Geophys. Res. Lett.*, **31**, L21105, doi:10.1029/2004GL020412.

McFarquhar, G.M., and H. Wang, 2006: Effects of aerosols on trade wind cumuli over the Indian Ocean: model simulations. *Quart. J. Roy. Meteor. Soc*.. In press.

Randall, D. A., Harshvardhan, and D. A. Dazlich, 1991: Diurnal variability of the hydrologic cycle in a general circulation model. *J. Atmos. Sci.,* **48**, 40–62.

Siebesma, A.P., and Coauthors, 2003: A large-eddy simulation intercomparison study of shallow cumulus convection. *J. Atmos. Sci.*, **60**, 1201-1219.

Smolarkiewicz, P.K., and L.G. Margolin, 1997: On forward-in-time differencing in fluids: An Eulerian /semi-Lagrangian nonhydrostatic model for stratified flows. *Atmosphere-Ocean*, **35**, 127-152.

Sommeria, G., 1976: Three-dimensional simulation of turbulent processes in an undisturbed tradewind boundary layer. *J. Atmos. Sci.,* **33**, 216–241.

Stevens, B., and Coauthors, 2001: Simulations of trade-wind cumuli under a strong inversion. *J. Atmos. Sci*, **58**,1870-1891.

Wood, R., C. S. Bretherton, and D. L. Hartmann, 2002: Diurnal cycle of liquid water path over the subtropical and tropical oceans. *Geophys. Res. Lett*., **29**, 2092, doi:10.1029/2002GL015371.